Influence of pressure and temperature on key physicochemical properties of corn stover-derived biochar

Manuel Azuara [a,*], Bárbara Baguer [b], José I. Villacampa [a], Niklas Hedin [c], Joan J. Manyà [d]

[a] Institute of Nanoscience of Aragón (INA), University of Zaragoza, Spain

[b] Technological College of Huesca, University of Zaragoza, Spain

[c] Department of Materials and Environmental Chemistry, Arrhenius Laboratory, Stockholm University, Sweden

[d] Aragón Institute of Engineering Research (I3A), University of Zaragoza, Spain

[*] Corresponding author: Manuel Azuara. E-mail address: mazuara@unizar.es

HIGHLIGHTS

- As-received corn stover was pyrolyzed as a means to avoid pre-treatment costs
- The effect of pressure was studied keeping the gas residence time constant
- Increasing the pressure led to a higher gas production at the expense of water
- The pressure had only a minor influence on the properties and yield of the biochar

ABSTRACT

This study focuses on analyzing the effect of both the peak temperature and pressure on the properties of biochar produced through slow pyrolysis of corn stover, which is a common agricultural waste that currently has little or no value. The pyrolysis experiments were carried out in a fixed-bed reactor at different peak temperatures (400, 525 and 650 °C) and absolute pressures (0.1, 0.85 and 1.6 MPa). The inert mass flow rate (at NTP conditions) was adjusted in each test to keep the gas residence time constant within the reactor. The as-received corn stover was pyrolyzed into a biochar without any physical pre-treatment as a way to reduce the operating costs. The properties of biochars showed that high peak temperature led to high fixed-carbon contents, high aromaticity and low molar H:C and O:C ratios; whereas a high pressure only resulted in a further decrease in the O:C ratio and a further increase in the fixed-carbon content. Increasing the operating pressure also resulted in a higher production of pyrolysis gas at the expense of water formation.

KEYWORDS

Corn stover, Pyrolysis, Biochar, Aromatic Carbon, Pressure

1. Introduction

Global warming is of worldwide concern and related to the anthropogenically enhanced concentrations of CO_2 and other greenhouse gases in the atmosphere. Previous studies have highlighted the positive effect of adding biochar to soil in terms of reducing such emissions to the atmosphere [1, 2]. Biochar can be produced by several thermochemical processes as conventional or slow pyrolysis which has been used to generate charcoal for many years [3, 4].

The production of biochar from corn stover appears to be a very promising alternative to integrate carbon sequestration measures and renewable energy generation into conventional agricultural production. Corn stover is the waste remaining in the field following the harvest of the grains. The corn production in Spain is about 4700 thousand tons per year [5]. Considering a waste yield of 0.65 (dry basis) and an average moisture content of 20 wt. % [6, 7], around 2440 thousand tons of corn stover are harvested per year in Spain.

Despite the fact that pyrolysis of biomass from agricultural or forest residues has been widely studied [3, 8], further research is strongly needed to fill the knowledge gaps related to how the operating conditions and feedstock affect the properties of biochar [9]. Typical operating conditions are the peak temperature, pressure, gas residence time, heating rate, atmosphere type, etc.

So far, very few studies have investigated how the operating conditions of pyrolysis influence the physicochemical properties of the corn stover-derived biochar. Fuertes et al. [10] reported that the biochar from corn stover pyrolysis at a peak temperature of 550 ºC was highly aromatic and had low H:C and O:C molar ratios (0.3 and 0.1, respectively). It was also reported by Enders et al. that both the H:C and O:C molar ratios decreased (from 0.9 to 0.4 and from 0.3 to 0.1, respectively) as the peak temperature was increased from

300 to 600 ºC [11]. Furthermore, and as observed for other types of biomass, the efficiency of carbonization was improved for large particles as compared with small, which led to charcoals with higher fixed-carbon contents [12]. This trend was related to the major role of the secondary charring reactions that occurred at the intra-particle level, which is highly relevant to industrial processes as it can contribute to saving costs in milling.

Previous investigations focused on producing charcoal from different lignocellulosic biomass have shown benefits of increasing the pressure used when it comes to both the charcoal and fixed-carbon yields [13-16]. The authors of those studies attributed this pressure effect to the enhanced kinetics of the secondary reactions of repolimerization and recondensation of the volatile matter during its contact with the solid matrix. However, this improvement in carbonization efficiency, as previously was stated by Manyà et al. [17], can also be related to an increase in the gas residence time within the pyrolysis reactor. In other words, the intrinsic effect of the pressure should be evaluated keeping constant the gas residence time of the inert carrier gas within the reactor.

The major goal of this study is to provide evidence on how the stability-related properties of the corn stover-derived biochars depend on both the temperature (pyrolysis peak temperature) and absolute pressure at a constant gas residence time. The effect on additional process variables, as for example the product distribution and the pyrolysis gas composition, was also investigated.

2. Materials and methods

2.1. Materials

The used corn stover (CS) contained corncob (15.5 wt. %), leaf (4.3 wt. %) and stalk (80.2 wt. %) that remained in the field following the harvest of cereal grain. It was supplied by a local farm located in the Spanish region of Aragón. The as-received CS was pyrolyzed without any previous crushing and sieving step. In this way, the thermochemical

conversion of this agricultural waste can be performed in a more cost-effective manner. The ranges of particle size for each fraction were: 1.5–10.0 cm long (stalk); 0.5–5.0 cm long (leaf); and 1.2–2.0 cm diameter and 2.0–5.0 cm long (corncob).

Proximate analyses were performed in quadruplicate according to ASTM standards (D3173 for moisture, D3174 for ash, and D3175 for volatile matter), whereas elemental analyses were carried out using a Leco TruSpec Micro CHNS analyzer (Leco Corporation, USA). Moreover, an ADVANT'XP+ XRF spectrometer (Thermo ARL, Switzerland) was used to measure the ash composition on the basis of the weight fractions of the equivalent oxides (according to ASTM standard D4326-04). Table 1 lists the results from the above-mentioned analyses.

2.2. Experimental system and procedure

The fixed-bed pyrolysis system consists of a cylindrical and vertical tube (140 mm inner diameter; 465 mm long) made of Sandvik 253 MA™ stainless steel. This reactor was heated by two electric resistances of 2.1 kW with proportional integral derivative (PID) temperature control. The total volume was 6 L and a basket of 4 L made of Monel™ alloy was used to put the biomass into the reactor. The temperature inside of the bed was measured using four thermocouples placed into a thermowell in different heights, three in contact with the bed (bottom, middle and top) and one in the freeboard (see Fig. S1 in Supplementary Information). A back pressure regulator was used to maintain the pressure of the system at a desired value. The produced gas passed through a hot filter and a heated line, maintained at a temperature of around 280 °C, before being passed through a series of two glass traps that were immerged in ice-water baths and followed by a filter (a glass tube filled with cotton wool pieces). A schematic diagram of the whole experimental set-up is shown in Fig. 1.

The pyrolysis tests were conducted in the fixed-bed reactor under an atmosphere of nitrogen gas, the mass flow rate at NTP conditions of which was adjusted as a function of the absolute pressure (0.1–1.6 MPa) and peak temperature (400–650 ºC) to maintain the real mass flow rate of nitrogen within the reactor at a constant value of 1.85 L min^{-1}. Thus, the N_2 mass flow applied was between 0.6 and 11.8 L NTP min^{-1} depending on the temperature and pressure conditions applied for a given pyrolysis run. During the experiments, the sample was heated at an average heating rate of 5 °C·min^{-1} up to the peak temperature with a soaking time of 1 h at this temperature. The initial sample weight was around 250 g, which represents around 90 % of the basket volume with a bed height of around 350 mm.

After each experiment, the biochar present in the reactor was collected and weighed. The pyrolysis liquid was recovered directly from the condensers without using any solvent as wash liquid. This glass trap was weighted before and after each experimental run to estimate the total liquid. Water content of the pyrolysis liquid was determined by Karl-Fischer titration (870 KF Titrino Plus, Manual Metrohm) with Hydranal Composite 5 as a titrant. The tar content of the pyrolysis liquid was determined by difference between the total liquid and the water content.

The composition of the major components in the pyrolysis gas (CO_2, CO, CH_4 and H_2) was determined using a Varian Micro GC CP-4900 gas chromatograph equipped with two analytical columns: a Molsieve 5A (molar sieves 5Å, 10 m length, using argon as carrier gas) and a PPQ (PolarPlot Q, 10 m length, using helium as carrier gas).

2.3. Product characterization

The mass yields of biochar, tar and water (y_{char}, y_{tar} and y_{water}, respectively) were calculated in a dry-ash-free (daf) basis. The biochars were characterized by proximate and elemental

composition analyses according to the same procedures described in section 2.1. The carbon retention in biochar after pyrolysis can be calculated as follows:

$$C\ retention(\%) = y_{char}\left(\frac{C_{char}}{C_{raw}}\right)100 \quad (1)$$

where C_{char} and C_{raw} are the carbon contents in a daf basis of biochar and feedstock, respectively.

As reported in earlier studies [11, 18], the fixed-carbon content of biochar is usually correlated with the molar H:C and O:C ratios as well as the aromaticity. In other words, the fixed-carbon content can be taken as a rough indicator of the potential stability of a given char in soil environments.

In addition, Singh et al. [19] observed a strong correlation between the degree of aromaticity (i.e., fraction of total carbon that is aromatic) and the carbon stability in soil. Both the direct polarization (DP) and cross-polarization (CP) techniques of solid-state ^{13}C NMR spectroscopy are well-established techniques for measuring the aromaticity of biochar [20-22]. Such DP and CP ^{13}C NMR spectra were recorded at a frequency of 100.6 MHz under conditions of magic angle spinning (MAS) of 14 kHz. For CP, a ramped (0.5 ms) contact pulse was used. SPINAL (small phase incremental alteration) decoupling of ^{1}H contributions were used during acquisition. Recycling delays of 2 s and 32 s were used and 32 k and 2 k scans were acquired for the CP and DP ^{13}C NMR measurements, respectively. A relatively moderate line broadening (150 Hz, exponential) was applied during Fourier transformation. From the experimental NMR spectra and according to McBeath et al. [23], the proportion of aromatic C was estimated as the ratio of the area under the aromatic peaks to the total area of the spectrum. A preliminary deconvolution procedure was carried out using the "Peak Analyzer" tool implemented in OriginPro version 9.05 (OriginLab, Northampton, MA). This deconvolution consisted of a nonlinear least-squares optimization

process where the experimental spectrum was described as the sum of multiple Gaussian peaks. The corresponding peaks were assigned as aromatic ones in the case that the center of the peak was in the chemical shift range of 120−160 ppm.

The specific surface area of the biochars was analyzed using N_2 physisorption data recorded at a temperature of −196 °C on a TriStar 3000 gas adsorption analyzer (Micromeritics, USA). The surface area (S_{BET}) was calculated using the Brunauer–Emmet–Teller (BET) model from adsorption data obtained at relatively low relative pressures (0.05–0.20). The average pore diameter (d_{avg}) was calculated from V_t and S_{BET}.

2.4. Statistical approach

A 2-level factorial design was adopted to study the effect of the two factors: peak temperature (400–650 °C) and pressure (0.1–1.6 MPa). Three replicates at the center point (525 °C and 0.85 MPa) were performed to simultaneously estimate the experimental error and the overall curvature effect [24]. A regression model including the linear and linear interaction terms was estimated for each response variable. Functional relationships between the response (y) and the coded independent variables (x_1, for peak temperature and x_2, for absolute pressure) are quantified by means of the estimated parameters of the regression model:

$$y = \beta_0 + \beta_1 x_1 + \beta_2 x_2 + \beta_{12} x_1 x_2 + \varepsilon \quad (2)$$

where β_0, β_j and β_{ij} are the intercept, linear and interaction coefficients; respectively. Statistical significance of the model terms was assessed by parametric tests (t-test). In the event that the overall curvature term is found to be significant (i.e., p-value < 0.05), the linear regression model is not fine enough and a second-order regression model with pure quadratic terms is probably required. To create the randomized design of experiments and perform the appropriate statistical analyses, the RcmdrPlugin.DoE package within the R environment (version 3.0.0) was used. Table 2 displays the created design.

3. Results and discussion

3.1. Product yields

The total mass balances between in- and output corn stover closed at values greater than 95%, with no apparent losses other than those occurring during normal lab scale processing (feeding, sampling, and collecting). The response variables related to the product yields and gas composition mentioned in section 2.3 were evaluated. The main results obtained and the statistical analyses from the factorial design of experiments are shown in Tables 3 and 4, respectively.

As expected, results from Table 4 clearly show that the biochar yield (y_{char}) decreased (at a 95% of confidence level) as the peak temperature of pyrolysis was higher. At this point, it is interesting to compare the results with similar and earlier studies. For instance, Liu et al. [25] reported a relatively low biochar yield (0.309) for the atmospheric slow pyrolysis of corn stalk at a peak temperature of 500 ºC. We must highlight that similar y_{char} values were reached at a higher peak temperature (i.e., 650 ºC) for the as-received feedstock and set-up used here. Our higher charcoal production could be due to the large particles used (Liu et al. used smaller particle sizes, in the range of 2–4 mm). As had been observed by Wang et al. [26] and Manyà et al. [17], an increased particle size leads to an increased residence time of the primary tar vapors within the particles, which causes an enhanced significance of the secondary charring reactions.

The effect of pressure on y_{char} was statistically negligible (see Table 4). This finding may seem to be in disagreement with some earlier studies that have reported a higher char production with an increased absolute pressure [14, 15, 27, 28]. However, we must emphasize that those studies were conducted at a constant mass flow rate of inert gas at NTP conditions and, thus, the gas residence time increased as the pressure rose.

Consequently, the observed increases in the char yield could exclusively be related to longer vapor-solid contact times.

The water and gas yields were significantly affected by the peak temperature and pressure. A high peak temperature or pressure led to a high gas yield at the expense of the yield of biochar (when the peak temperature was high) or water (when the pressure was high). The increased gas yield on an increased peak temperature was expected because of the thermodynamically and kinetically favored devolatilization process [29]. Moreover, an increased temperature can lead to an enhancement of the secondary cracking reactions, given the relatively high residence time of the pyrolysis vapors. However, the effect of pressure on the product distribution (i.e., statistically significant increase in gas yield and the expense of water) needs to be discussed in detail. As suggested by previous studies [30, 31], the vapor pressure of the precursors of tar increases with the absolute pressure, which results in enhanced cross-linking reactions leading to the formation of char and gas at relatively low temperatures. At higher temperatures, however, the steam-char gasification reaction could become relevant during pressurized pyrolysis experiments. In this context, Matsuoka et al. [31] observed a significant increase in the steam gasification reaction rate when the partial pressure of the gasifying agent increased in the range of 0.1−0.5 MPa, for coal gasification in a fluidized bed. Moreover, a catalytic effect of the inherent alkali and alkaline earth metallic (AAEM) species on the steam gasification of char has been observed [32-34]. As can be seen in Table 1, Ca and, to a lesser extent, K, are noticeably present in the corn stover samples. The hypothetical enhancement of the steam gasification reaction with an increased pressure can thus explain two observed findings: (i) the lower water yield and (ii) the negligible effect on the char yield. Biochar formation is favored due to the restricted transport of volatiles but, at the same time, some carbon could be gasified by reaction with steam.

Concerning the tar yield, no statistically significant effects of the two analyzed factors were observed (see Table 4). As a general trend, when a higher peak temperature is used a higher biomass decomposition could be expected. In such cases, more volatiles could be produced and, consequently, the tar yield could be increased as compared with pyrolysis conducted at a lower peak temperature. However, our results do not support such a hypothesis. A possible explanation to the deviation is that the extent of the secondary cracking reactions was enhanced when the peak temperature was increased during pyrolysis. We must also remark that the experimental setup used here can allow an additional thermal cracking of volatiles in the vapor phase due to the relatively high residence time of the pyrolysis vapors in the freeboard area.

The axial temperature profiles and the release rates of the four main gas components (CO_2, CO, CH_4 and H_2) are given in Supplementary Information. Note that the axial temperature gradients were very high for the specific pyrolysis runs conducted under atmospheric pressure (see Figs. S2 and S4). As the pressure was increased, the temperature became more homogeneous along the packed bed (see Figs S3 and S5), as a consequence of the enhanced convective heat transfer due to the higher N_2 mass flow rate (at NTP conditions) that passed through the reactor. For the gas release rates, the shape and magnitude of the peaks shown in Figs. S2–S6 depend on the severity in heating conditions and working pressure. However, these differences may depend on numerous factors. Instead of speculating on the dependencies, we analyzed how the selected factors affected the cumulative yields of the gas species. Given the results listed in Table 4, it is clear that an increase in temperature from 400 to 650 °C led to an increase in the yields of all gases mainly due to an enhancement of the thermal cracking of the primary volatiles. To a lesser extent, the higher y_{gas} values can be related to the higher degradation of lignin, which actively takes place at temperatures of 327–477 °C [35]. The enhanced production of H_2 at

higher temperatures could be also explained by contributions from the water-gas shift reaction in the gas phase, as has recently been observed by Hu et al. [36]. For its part, an increase in the pressure led to a significant increase in the yields of CO_2 and CO. As has recently been observed by Qian et al. [37], a high absolute pressure could promote the decarboxylation of the hemicellulole and cellulose, leading to cross-linking reactions and an increased release of CO_2. The increase in the yield of CO could be explained by (i) the above-mentioned enhancement of the steam gasification reaction with an increased pressure, and (ii) a promotion of decarbonylation reactions under elevated pressure. Unexpectedly, the cumulative yield of CH_4 did not significantly increase with pressure applied (*p-value* = 0.49), despite the thermodynamically favored methanation reactions.

3.2 The properties of biochar

Table 5 displays the main results obtained from the factorial design of experiments for the response variables related to the properties of produced biochar. As can be seen from Table 6, the regression model for *C retention* did not describe the data well (R^2_{adj} = 0.647), revealing that, for the evaluated range of operating conditions, neither peak temperature nor pressure have a major impact on the carbon retention. The statistically not significant effect of the peak temperature on *C retention* was somewhat expected, since an increased temperature causes an increase in the content of carbon but a simultaneous decrease in the biochar yield. In regard to the effects on the H:C molar ratio, significant changes were only observed for the peak temperature, whereas both analyzed factors significantly affect the O:C molar ratio. The observed decreases in both molar ratios when the peak temperature increased are in good agreement with previous results reported in the literature [38, 39].

In addition to the significant decrease in both the H:C and O:C ratios, a clear increase in the fixed-carbon content, the percentage of aromatic C and the BET specific surface area were observed when the peak temperature was at the highest level (see Table 6). In

addition, a high pressure led to a further increase in the fixed-carbon content and a further decrease in the O:C molar ratio. These dependencies were probably related to the enhancement of decarboxylation reactions of the hemicellulose and cellulose, leading to a decrease in the oxygen content of the biochar [40]. An additional explanation could be that an increased pressure could promote the loss of oxygenated functional groups during the secondary cracking reactions. In this sense, Yang et al. [41] reported a noticeable loss of oxygenated functional groups in the surface of char during the pyrolysis of coal at pressures of 0.8 MPa and above. However, the effect of pressure was negligible on the H:C ratio as well as on the aromaticity.

It should be pointed out that several response variables had a significant curvature term (*p-values* lower than 0.05). In order to provide more accurate regression models for these variables (*O:C ratio*, *% FC*, *Aromatic C*, S_{BET}, and d_{avg}), extended central composite designs of experiments would be required.

With regard to the aromatic C present in the biochar, Fig. 2 displays the CP/MAS ^{13}C NMR spectra for a range of different chars prepared from corn stover at 400 and 525 ºC. The biochar obtained at 400 ºC and 0.1 MPa (run 6) displays an intense broad band at a ^{13}C chemical shift of ~128 ppm, typical for aromatic groups (and some other moieties) [42-44]. Non-oxygenated aliphatic moieties are detected by the bands in the region of 10–50 ppm. Note that CP/MAS ^{13}C NMR can only be used qualitatively when it comes to this class of solids. It will overestimate the amount of non-aromatic carbons. However, a clear band of the CH_2-O in cellulose was detected at a chemical shift of 74 ppm [42, 45]. For the biochar produced at a peak temperature of 400 ºC and an absolute pressure of 1.6 MPa (run 2) most of the aliphatic bands were absent from the spectrum. For the conditions corresponding to the center point (525 °C and 0.85 MPa) only a small fraction of aliphatic compounds were detected (see Fig. 2 for runs 1, 4 and 5). For biochars produced at 650 ºC, it was not

possible to conduct the CP/MAS measurements with our set up due to a more conductive structure. Alternative DP ^{13}C NMR spectra were obtained for high-temperature biochars (see Fig. 3), showing a high degree of aromatization (the percentages of aromatic C reached values higher than 83% for biochars produced at 650 ºC). This finding is in line with the results reported in previous studies, in which a higher aromaticity was measured when pyrolysis temperature increased [17, 19, 46-49]. As a general rule, the aromatic character of the biochar is accentuated due to a continuous loss of hydroxyl and aliphatic groups, as successively higher pyrolysis temperatures are used [40].

The non-statistically significant effect of pressure on the aromaticity is in agreement with previous studies using other biomass sources (vine shoots [17] and olive mill waste [49]). Nevertheless and as recently stated by Guo and Chen [50], the stability of biochars is not only determined by aromatic structures but also influenced by possible interactions between carbon and inorganic constituents and particle size. In other words, further investigations focused on analyzing the oxidation kinetics of biochar in both the short and long term are required to assess definitely the effect of pressure on the stability of biochars.

In order to provide additional insights into the possible correlation among the response variables (fixed-carbon content, molar H:C and O:C ratios, and proportion of aromatic C) related to the potential stability, Fig. 4 shows the bi-plot based on the principal component analysis (PCA). From this plot and in line with the above-mentioned considerations, it is clear that the peak temperature has a stronger influence than pressure on the potential stability of the biochar derived from corn stover by slow pyrolysis. When operating at the highest peak temperature, the pyrolysis led to high fixed-carbon contents and aromaticity and low molar H:C and O:C ratios. An increase in pressure only resulted in an additional decrease in the O:C ratio and an additional increase in the fixed-carbon content. From Fig. 4, it is clear that the fixed-carbon content and the H:C ratio were highly linearly correlated.

Concerning the BET specific surface area, a moderate increase in the peak temperature from 400 to 525 ºC led to a product with a higher porosity, which developed mainly as a microporosity (pores < 2 nm in size) given the parallel decrease in the average pore diameter. This result is in reasonable agreement with those reported in earlier studies about pyrolysis at atmospheric pressure of straw and lignosulfonate [51] or rice husk, rice straw and wood chips of apple tree [52]. However, the BET specific surface areas for biochars produced at 525 ºC and 650 ºC were quite similar. Some authors have attributed this tendency to the higher ash content of the high-temperature chars resulting in a possible blockage of micropores [53, 54].

4. Conclusions

Based on the results from the present study, the following conclusions are drawn:

(1) In addition to the expected effects of the peak temperature on the product distribution from the pyrolysis, an increase in the operating pressure led to a higher production of gas at the expense of water. This could be explained by two concurrent reasons: (i) enhanced contributions from cross-linking reactions due to increased vapor pressures of volatiles and (ii) a contribution from the steam-char gasification reaction.

(2) The negligible effect of pressure on the yield of biochar, when the superficial velocity of the inert gas was kept constant, confirmed that the effect of the vapor residence time within the pyrolysis reactor on the biochar yield is greater than that of pressure.

(3) The large particle size of the corn stover used here can explain the overall excellent results obtained on the key carbonization efficiency indicators: high fixed-carbon contents (78.7%–90.4%), low molar H:C ratios (0.25–0.59) and O:C ratios (0.06–0.15), and high percentages of aromatic C (68.6%–83.8%).

(4) An increase in the peak temperature used during pyrolysis led to a high fixed-carbon content and aromaticity and low molar H:C and O:C ratios, whereas an increase in the pressure only resulted in a further decrease in the O:C ratio and a further increase in the fixed-carbon content. Further studies (e.g., those determining the oxidation behavior of the biochars produced at different pressures) are required to definitively evaluate the appropriateness of using pressurized pyrolysis systems for biochar production purposes.

Nomenclature

C_{char}	carbon content of biochar in a daf basis
C_{raw}	carbon content of feedstock in a daf basis
d_{avg}	average pore diameter (nm)
%FC	fixed-carbon content in a daf basis
m_{char}	mass of produced char (g)
m_{raw}	dry mass of raw material (g)
R^2_{adj}	adjusted coefficient of determination
S_{BET}	Brunauer–Emmet–Teller specific surface area ($m^2\ g^{-1}$)
T_{peak}	pyrolysis peak temperature (°C)
V_t	total volume pore ($cm^3\ g^{-1}$)
x_1	coded variable for peak temperature
x_2	coded variable for absolute pressure
y_{char}	biochar yield (kg kg^{-1} of biomass in a daf basis)
y_{gas}	gas yield in a dry basis (kg kg^{-1} of biomass in a dry ash and N_2-free basis)
y_{tar}	yield of producer gas (kg kg^{-1} of biomass in a daf basis)
y_{water}	yield of producer gas (kg kg^{-1} of biomass in a daf basis)

Greek Symbols

β_0	regression coefficient for the intercept term
β_1	regression coefficient for the linear effect of peak temperature
β_2	regression coefficient for the linear effect of absolute pressure
β_{12}	regression coefficient for the interaction term

Acronyms

BET	Brunauer Emmett Teller

CP MAS ^{13}C NMR	Cross-Polarization Magic Angle Spinning Carbon-13 Nuclear Magnetic Resonance.
DP ^{13}C NMR	Direct Polarization Carbon-13 Nuclear Magnetic Resonance
XRF	X-ray fluorescence

Table 1

Proximate, elemental and XRF analyses of corn stover

Proximate (wt. %)	
Ash	2.50 ± 0.20
Moisture	7.27 ± 0.31
Volatile matter	80.3 ± 0.11
Fixed carbon	9.93 ± 0.49
Elemental (wt.%, daf basis)	
C	44.4 ± 0.31
H	5.60 ± 0.04
N	0.43 ± 0.01
S	0.45 ± 0.05
Inorganic matter (wt.% of ash)	
SiO_2	31.41± 0.23
CaO	30.71± 0.23
K_2O	9.85± 0.15
Fe_2O_3	6.49± 0.12
Al_2O_3	4.85± 0.12
P_2O_5	4.13± 0.10
MgO	3.45± 0.17
PbO	2.50± 0.08
S	1.94± 0.07
Cl	0.594±0.030
TiO_2	0.586± 0.029
MnO	0.526± 0.026
SnO_2	0.450 ± 0.034
ZnO	0.240± 0.021
SrO	0.199± 0.021
Cr_2O_3	0.178 ± 0.023
CuO	0.081± 0.024

Table 2

Matrix of the factorial design adopted to analyze the pyrolysis of corn stover

Level	Factors	
	x_1	x_2
	Peak temperature, T_{peak} (°C)	Pressure, P (MPa)
Low (−1)	400	0.1
Middle (0)	525	0.85
High (+1)	650	1.6
Run	Factors	
	x_1	x_2
1	0	0
2	−1	+1
3	+1	+1
4	0	0
5	0	0
6	−1	−1
7	+1	−1

Table 3

Yields of pyrolysis products (kg kg^{-1} daf feedstock) and main gas compounds (mmol g^{-1} daf feedstock) as a function of pressure and peak temperature

Run	y_{char}	y_{tar}	y_{water}	y_{gas}	CO_2	CO	CH_4	H_2
6 (–1, –1)	0.375	0.172	0.210	0.243	2.56	1.35	0.142	0.076
7 (+1, –1)	0.301	0.174	0.222	0.302	2.94	2.06	1.30	1.55
1 (0, 0)	0.320	0.193	0.147	0.340	4.05	1.66	0.981	0.710
4 (0, 0)	0.300	0.164	0.181	0.355	4.05	1.71	0.895	0.699
5 (0, 0)	0.308	0.184	0.155	0.353	4.25	1.67	0.740	0.506
2 (–1, +1)	0.362	0.158	0.110	0.370	2.94	1.33	0.207	0.051
3 (+1, +1)	0.284	0.166	0.123	0.427	3.71	2.60	1.44	1.74

Table 4.

Summary statistics for the regression models based on the data given in Table 3 (values in brackets correspond to the *p-values* resulting from the hypothesis tests)

Response	β_0	β_1	β_2	β_{12}	*Curvature*[a]	R^2_{adj}[b]
y_{char}	0.330	–0.038 **(0.017)**	–0.015 (0.275)	–0.001 (0.861)	–0.021 (0.110)	0.913
y_{tar}	0.168	0.002 (0.768)	–0.006 (0.536)	0.002 (0.859)	0.013 (0.375)	0.000
y_{water}	0.166	0.006 (0.555)	–0.050 **(0.030)**	0.000 (0.980)	–0.005 (0.736)	0.823
y_{gas}	0.336	0.029 **(0.019)**	0.063 **(0.004)**	0.000 (0.914)	0.014 (0.156)	0.980
CO_2 (mmol g^{-1} feedstock)	3.038	0.288 **(0.038)**	0.288 **(0.038)**	0.098 (0.233)	1.079 **(0.007)**	0.971
CO (mmol g^{-1} feedstock)	1.835	0.495 **(0.001)**	0.130 **(0.010)**	0.140 **(0.009)**	–0.155 **(0.017)**	0.996
CH_4 (mmol g^{-1} feedstock)	0.772	0.598 **(0.010)**	0.051 (0.490)	0.019 (0.788)	0.100 (0.397)	0.940
H_2 (mmol g^{-1} feedstock)	0.854	0.791 **(0.005)**	0.041 (0.543)	0.054 (0.443)	–0.275 (0.087)	0.971

[a] Regression coefficient for the overall curvature term

[b] Calculated for the regression model that includes the curvature term

Table 5

Results of the design of experiments adopted to analyze the biochar properties from corn stover pyrolysis

Run	C retention (%)	H:C molar ratio	O:C molar ratio	*%FC*	Aromatic C (%)	S_{BET} ($m^2\ g^{-1}$)	d_{avg} (nm)
6 (−1, −1)	60.47	0.589	0.154	78.72	71.04	1.437	7.423
7 (+1, −1)	51.15	0.246	0.128	82.94	83.80	160.9	1.006
1 (0, 0)	58.14	0.381	0.059	88.76	68.85	184.9	0.997
4 (0, 0)	53.90	0.403	0.062	87.91	72.09	182.8	1.240
5 (0, 0)	55.14	0.394	0.062	87.46	68.59	140.9	1.267
2 (−1, +1)	59.88	0.580	0.122	80.93	69.32	3.904	5.066
3 (+1, +1)	52.46	0.256	0.063	90.43	83.49	172.4	1.366

Table 6

Summary statistics for the regression models based on the data given in Table 5 (values in brackets correspond to the *p-values* resulting from the hypothesis tests)

Response	β_0	β_1	β_2	β_{12}	*Curvature*[a]	R^2_{adj}[b]
C retention (%)	55.99	–4.185	0.180	0.475	–0.263	0.647
		(0.062)	(0.884)	(0.706)	(0.889)	
H:C molar ratio	0.418	–0.167	0.000	0.005	–0.025	0.994
		(0.001)	(0.968)	(0.481)	(0.097)	
O:C molar ratio	0.117	–0.021	–0.024	–0.008	–0.056	0.998
		(0.002)	**(0.001)**	**(0.011)**	**(0.001)**	
%FC	83.26	3.430	2.425	1.320	4.788	0.978
		(0.009)	**(0.018)**	(0.057)	**(0.011)**	
Aromatic C (%)	76.91	6.732	–0.508	0.353	–7.069	0.917
		(0.020)	(0.655)	(0.752)	**(0.042)**	
S_{BET} *(m² g⁻¹)*	84.66	81.99	3.492	2.258	84.87	0.891
		(0.022)	(0.805)	(0.872)	**(0.046)**	
d_{avg} *(nm)*	3.715	–2.529	–0.499	0.679	–2.547	0.997
		(0.001)	**(0.021)**	**(0.012)**	**(0.002)**	

[a] Regression coefficient for the overall curvature term.

[b] Calculated for the regression model that includes the curvature term

.

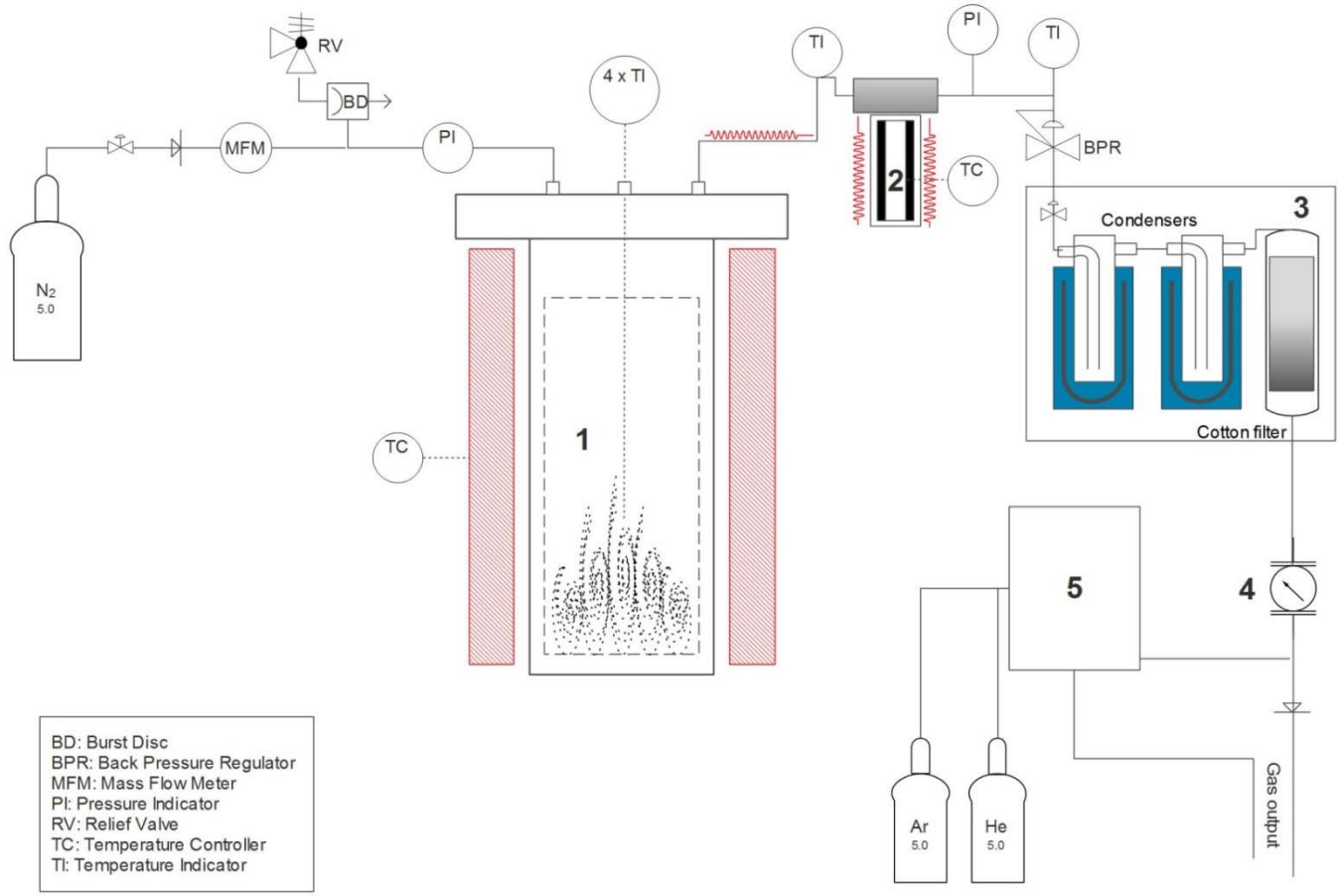

Fig.1. Schematic layout of the experimental setup: (1) fixed-bed pyrolysis reactor, (2) hot filter, (3) pyrolysis liquid condensation system, (4) volumetric gas meter and (5) μ-GC.

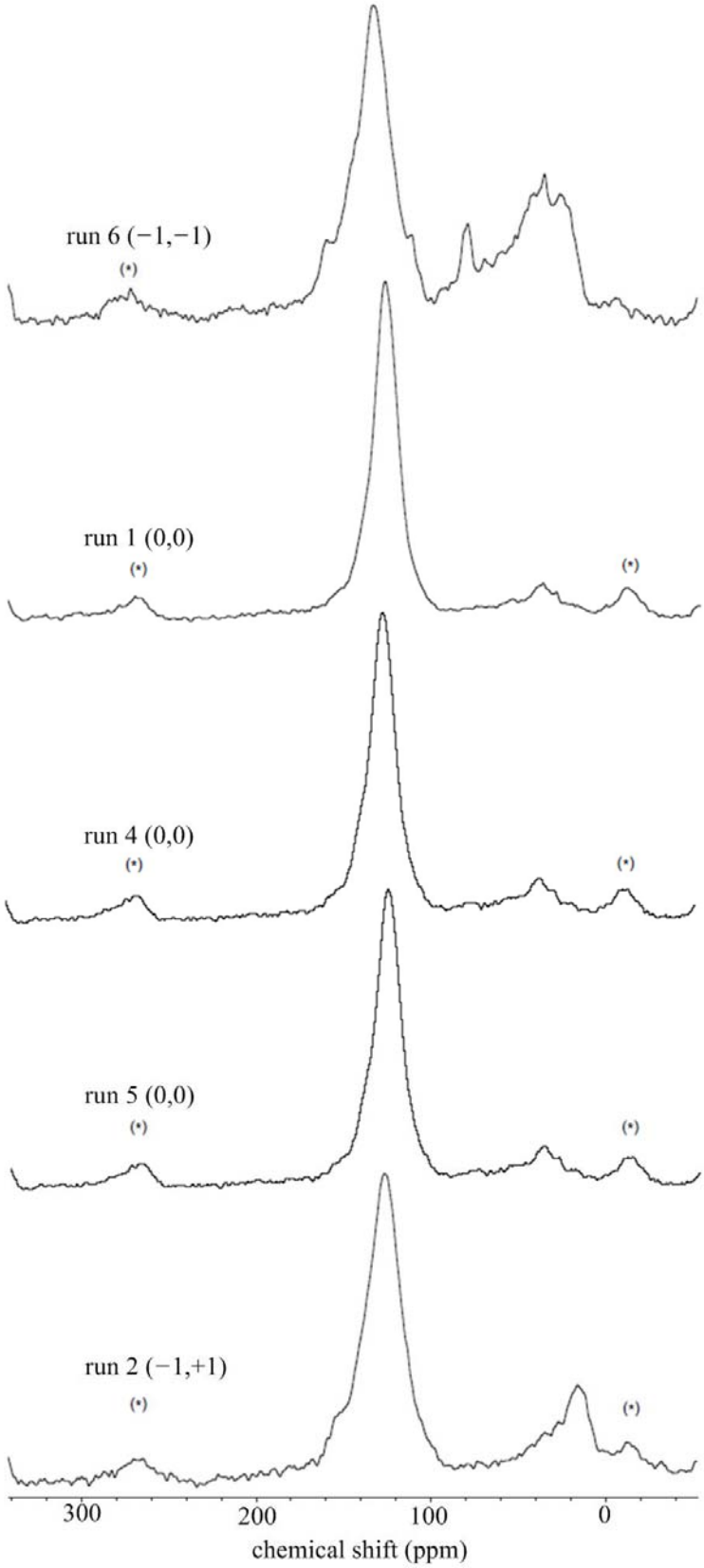

Fig 2. Solid state CP/MAS ^{13}C NMR spectra of the biochars obtained in run 6 (−1, −1); runs 1, 4, 5 (0,0); and run 2 (−1, +1).

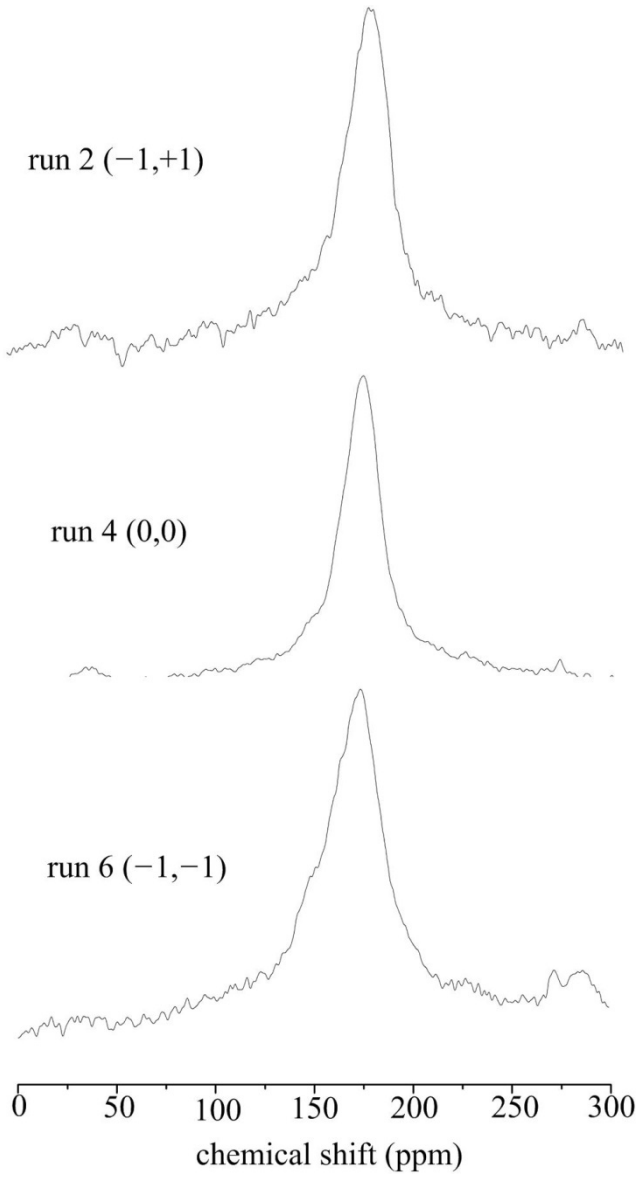

Fig. 3. Solid state DP ^{13}C NMR spectra of the biochars obtained in runs 2 (−1,+1); 4 (0,0); and 6 (−1, −1).

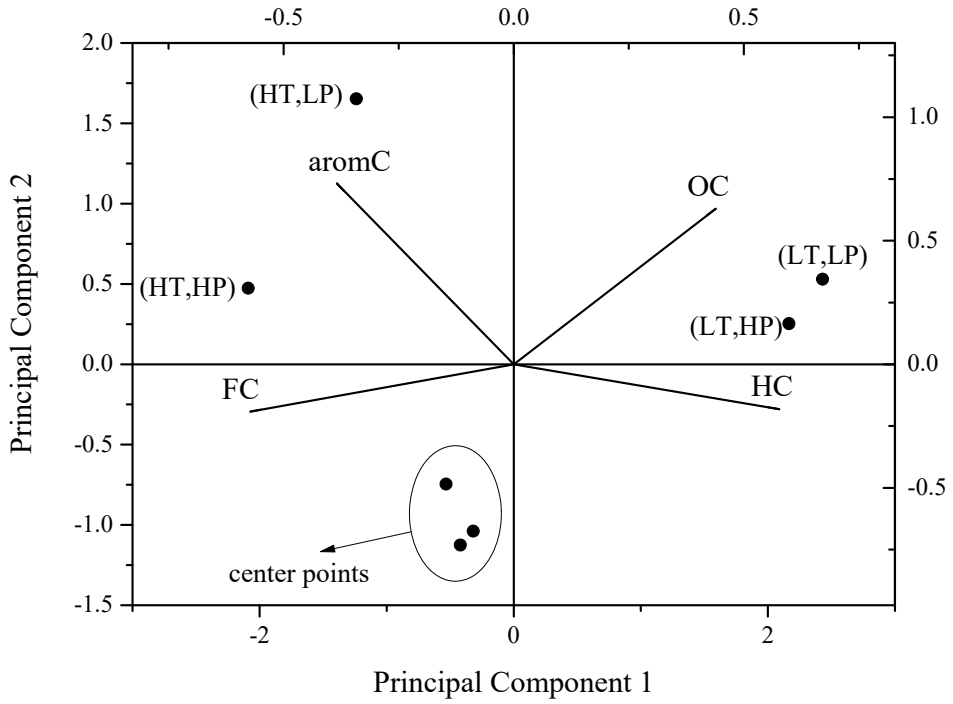

Fig. 4. Bi-plot obtained through principal component analysis (PCA). The two first PCs account for 96.9% of the total variation in the dependency structure of the four variables related to the potential stability of biochar (FC: fixed-carbon content, aromC: proportion of aromatic C, HC: molar H:C ratio, OC: molar O:C ratio) (HT: high-temperature, LT: low temperature, HP: high pressure, LP: low pressure).

Acknowledgements

The authors wish to acknowledge financial support from the Spanish MINECO-DGI (Project ENE2013-47880-C3-1-R). JJM also express his gratitude to the Aragon Government (GPT group) and the European Social Fund for additional financial support.

References

[1] Lehmann J, Joseph S. Biochar for environmental management. Science and Technology, London, Sterling, VA: Earthscan; 2009.
[2] Fowles M. Black carbon sequestration as an alternative to bioenergy. Biomass Bioenergy 2007;31:426-32.
[3] Sohi S, Loez-Capel E, Krull E, Bol R. Biochar's roles in soil and climate change: A review of research needs. CSIRO Land and Water Science Report 2009:1-56.
[4] Yoshida T, Antal MJ. Sewage sludge carbonization for terra preta applications. Energy Fuel 2009;23:5454−9.
[5] Eurostat. Agricultural production - crops, 2015. Available from: http://ec.europa.eu/eurostat/statistics-explained/index.php/Agricultural_production_-_crops
[6] Di Blasi C, Tanzi V, Lanzetta M. A study on the production of agricultural residues in Italy. Biomass Bioenergy 1997;12:321-31.
[7] Pordesimo LO, Edens WC, Sokhansanj S. Distribution of aboveground biomass in corn stover. Biomass Bioenergy 2004;26:337-43.
[8] Krull ES, Skjemstad JO, Baldock JA. Functions of soil organic matter and the effect on soil properties. Report for GRDC and CRC for Greenhouse Accounting. CSIRO Land and Water Client Report 2004.
[9] Zhang L, Xu C, Champagne P. Overview of recent advances in thermo-chemical conversion of biomass. Energy Convers Manage 2010;51:969-82.
[10] Fuertes AB, Arbestain MC, Sevilla M, Maciá-Agulló JA, Fiol S, López R, Smernik RJ, Aitkenhead WP, Arce F, Macias F. Chemical and structural properties of carbonaceous products obtained by pyrolysis and hydrothermal carbonisation of corn stover. Soil Research 2010;48:618-26.
[11] Enders A, Hanley K, Whitman T, Joseph S, Lehmann J. Characterization of biochars to evaluate recalcitrance and agronomic performance. Bioresour Technol 2012;114:644-53.
[12] Hanwu L, Shoujie R, James J. The effects of reaction temperature and time and particle size of corn stover on microwave pyrolysis. Energy Fuels 2009;23:3254-61.
[13] Antal MJ, Croiset E, Dai X, De Almeida C, Mok WSL, Norberg N, Richard JR, Al Majthoub M. High-yield biomass charcoal. Energy Fuels 1996;10:652-8.

[14] Várhegyi G, Szabó P, Till F, Zelei B, Antal MJ, Dai X. TG, TG-MS, and FTIR characterization of high-yield biomass charcoals. Energy Fuels 1998;12:969-74.
[15] Antal MJ, Allen SG, Dai X, Shimizu B, Tam MS, Grønli M. Attainment of the theoretical yield of carbon from biomass. Ind Eng Chem Res 2000;39:4024-31.
[16] Mahinpey N, Murugan P, Mani T, Raina R. Analysis of bio-oil, biogas, and biochar from pressurized pyrolysis of wheat straw using a tubular reactor. Energy Fuels 2009;23:2736-42.
[17] Manyà JJ, Ortigosa MA, Laguarta S, Manso JA. Experimental study on the effect of pyrolysis pressure, peak temperature, and particle size on the potential stability of vine shoots-derived biochar. Fuel 2014;133:163-72.
[18] Manyà JJ. Pyrolysis for biochar purposes: A review to establish current knowledge gaps and research needs. Environ Sci Technol 2012;46:7939-54.
[19] Singh BP, Cowie AL, Smernik RJ. Biochar carbon stability in a clayey soil as a function of feedstock and pyrolysis temperature. Environ Sci Technol 2012;46:11770-8.
[20] Barron PF, Wilson MA. Humic soil and coal structure study with magic-angle spinning 13C CP-NMR. Nature 1981;289:275-6.
[21] Tekely P, Nicole D, Brondeau J, Delpuech JJ. Application of carbon-13 solid-state high-resolution NMR to the study of proton mobility. Separation of rigid and mobile components in coal structure. The Journal of Physical Chemistry 1986;90:5608-11.
[22] Wooten JB, Seeman JI, Hajaligol MR. Observation and Characterization of Cellulose Pyrolysis Intermediates by 13C CPMAS NMR. A New Mechanistic Model. Energy Fuels 2004;18:1-15.
[23] McBeath A, Smernik R, Plant E. Determination of the aromaticity and the degree of aromatic condensation of a thermosequence of wood charcoal using NMR. Organic Geochemistry 2011;42:1194-202.
[24] Montgomery DC. Design and analysis of experiments. Hoboken 6th: John Wiley & Sons.
[25] Liu X, Zhang Y, Li Z, Feng R, Zhang Y. Characterization of corncob-derived biochar and pyrolysis kinetics in comparison with corn stalk and sawdust. Bioresour Technol 2014;170:76-82.
[26] Wang L, Skreiberg Ø, Gronli M, Specht GP, Antal MJ. Is Elevated Pressure Required to Achieve a High Fixed-Carbon Yield of Charcoal from Biomass? Part 2: The Importance of Particle Size. Energy Fuels 2013;27:2146-56.
[27] Recari J, Berrueco C, Abelló S, Montané D, Farriol X. Effect of temperature and pressure on characteristics and reactivity of biomass-derived chars. Bioresour Technol 2014;170:204-10.
[28] Noumi ES, Blin J, Valette J, Rousset P. Combined Effect of Pyrolysis Pressure and Temperature on the Yield and CO2 Gasification Reactivity of Acacia Wood in macro-TG. Energy Fuels 2015;29:7301-8.
[29] Di Blasi C, Signorelli G, Di Russo C, Rea G. Product Distribution from Pyrolysis of Wood and Agricultural Residues. Ind Eng Chem Res 1999;38:2216-24.
[30] Ragucci R, Giudicianni P, Cavaliere A. Cellulose slow pyrolysis products in a pressurized steam flow reactor. Fuel 2013;107:122-30.
[31] Matsuoka K, Ma Z-X, Akiho H, Zhang Z-G, Tomita A, Fletcher TH, Wójtowicz MA, Niksa S. High-Pressure Coal Pyrolysis in a Drop Tube Furnace. Energy Fuels 2003;17:984-90.

[32] Yip K, Tian F, Hayashi J-i, Wu H. Effect of Alkali and Alkaline Earth Metallic Species on Biochar Reactivity and Syngas Compositions during Steam Gasification. Energy Fuels 2010;24:173-81.
[33] Dupont C, Nocquet T, Da Costa Jr JA, Verne-Tournon C. Kinetic modelling of steam gasification of various woody biomass chars: Influence of inorganic elements. Bioresour Technol 2011;102:9743-8.
[34] Nanou P, Gutiérrez Murillo HE, van Swaaij WPM, van Rossum G, Kersten SRA. Intrinsic reactivity of biomass-derived char under steam gasification conditions-potential of wood ash as catalyst. Chemical Engineering Journal 2013;217:289-99.
[35] Branca C, Albano A, Di Blasi C. Critical evaluation of global mechanisms of wood devolatilization. Thermochimica Acta 2005;429:133-41.
[36] Hu S, Jiang L, Wang Y, Su S, Sun L, Xu B, He L, Xiang J. Effects of inherent alkali and alkaline earth metallic species on biomass pyrolysis at different temperatures. Bioresour Technol 2015;192:23-30.
[37] Qian Y, Zhang J, Wang J. Pressurized pyrolysis of rice husk in an inert gas sweeping fixed-bed reactor with a focus on bio-oil deoxygenation. Bioresour Technol 2014;174:95-102.
[38] Ghani WAWAK, Mohd A, da Silva G, Bachmann RT, Taufiq-Yap YH, Rashid U, Al-Muhtaseb AH. Biochar production from waste rubber-wood-sawdust and its potential use in C sequestration: Chemical and physical characterization. Industrial Crops and Products 2013;44:18-24.
[39] Wu W, Yang M, Feng Q, McGrouther K, Wang H, Lu H, Chen Y. Chemical characterization of rice straw-derived biochar for soil amendment. Biomass Bioenergy 2012;47:268-76.
[40] Sharma RK, Wooten JB, Baliga VL, Lin X, Geoffrey Chan W, Hajaligol MR. Characterization of chars from pyrolysis of lignin. Fuel 2004;83:1469-82.
[41] Yang H, Chen H, Ju F, Yan R, Zhang S. Influence of Pressure on Coal Pyrolysis and Char Gasification. Energy Fuels 2007;21:3165-70.
[42] David K, Pu Y, Foston M, Muzzy J, Ragauskas A. Cross-Polarization/Magic Angle Spinning (CP/MAS) 13C Nuclear Magnetic Resonance (NMR) Analysis of chars from alkaline-treated pyrolyzed softwood. Energy Fuels 2009;23:498-501.
[43] Schnitzer MI, Monreal CM, Facey GA, Fransham PB. The conversion of chicken manure to biooil by fast pyrolysis I. Analyses of chicken manure, biooils and char by 13C and 1H NMR and FTIR spectrophotometry. J Environ Sci Health, Part B 2007;42:71-7.
[44] Calkins W, Hagaman E, Zeldes H. Coal flash pyrolysis: 1. An indication of the olefin precursors in coal by CP/MAS 13C n.m.r. spectroscopy. Fuel 1984;63:1113-8.
[45] Hao W, Björkman E, Yun Y, Lilliestråle M, Hedin N. Iron oxide nanoparticles embedded in activated carbons prepared from hydrothermally treated waste biomass. ChemSusChem 2014;7:875-82.
[46] Nguyen BT, Lehmann J, Hockaday WC, Joseph S, Masiello CA. Temperature sensitivity of black carbon decomposition and oxidation. Environ Sci Technol 2010;44:3324-31.
[47] McBeath AV, Smernik RJ, Krull ES, Lehmann J. The influence of feedstock and production temperature on biochar carbon chemistry: A solid-state 13C NMR study. Biomass Bioenergy 2014;60:121-9.

[48] Wiedemeier DB, Abiven S, Hockaday WC, Keiluweit M, Kleber M, Masiello CA, McBeath AV, Nico PS, Pyle LA, Schneider MPW, Smernik RJ, Wiesenberg GLB, Schmidt MWI. Aromaticity and degree of aromatic condensation of char. Organic Geochemistry 2015;78:135-43.
[49] Manyà JJ, Laguarta S, Ortigosa MA, Manso JA. Biochar from Slow Pyrolysis of Two-Phase Olive Mill Waste: Effect of Pressure and Peak Temperature on its Potential Stability. Energy Fuels 2014;28:3271-80.
[50] Guo J, Chen B. Insights on the Molecular Mechanism for the Recalcitrance of Biochars: Interactive Effects of Carbon and Silicon Components. Environ Sci Technol 2014;48:9103-12.
[51] Zhang J, Liu J, Liu R. Effects of pyrolysis temperature and heating time on biochar obtained from the pyrolysis of straw and lignosulfonate. Bioresour Technol 2015;176:288-91.
[52] Jindo K, Mizumoto H, Sawada Y, Sanchez-Monedero MA, Sonoki T. Physical and chemical characterization of biochars derived from different agricultural residues. Biogeosciences 2014;11:6613-21.
[53] Mackay DM, Roberts PV. The influence of pyrolysis conditions on yield and microporosity of lignocellulosic chars. Carbon 1982;20:95-104.
[54] Song W, Guo M. Quality variations of poultry litter biochar generated at different pyrolysis temperatures. J Anal Appl Pyrolysis 2012;94:138-45.